

# Synthesis and spectroscopic properties of diorganotin(IV) derivatives of 2,6-diacetylpyridine bis(thiosemicarbazone). Crystal structure of diphenyl{2,6-diacetylpyridine bis(thiosemicarbazonato)}tin(IV) bis(dimethylformamide) solvate

J.S. Casas\*, A. Castiñeiras, A. Sánchez, J. Sordo and A. Vázquez-López

*Departamento de Química Inorgánica, Universidade de Santiago de Compostela, 15706 Santiago de Compostela (Spain)*

M.C. Rodríguez-Argüelles

*Departamento de Química Pura e Aplicada, Universidade de Vigo, 36200 Vigo (Spain)*

U. Russo

*Dipartimento di Chimica Inorganica, Metallorganica ed Analitica, Università di Padova, 35131 Padua (Italy)*

(Received November 15, 1993; revised January 31, 1994)

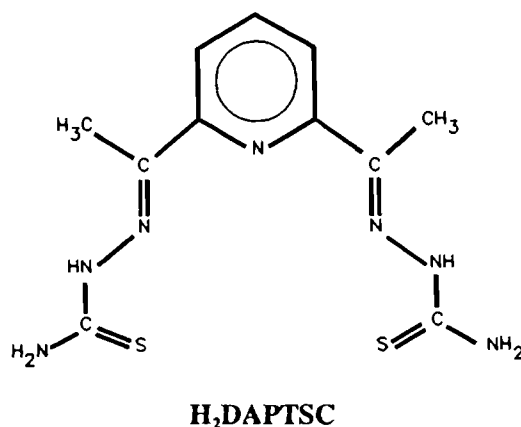
## Abstract

The reaction of the title ligand ( $H_2DAPTSC$ ) with  $SnR_2O$  ( $R=Me, Ph$ ) in DMF afforded the complexes  $[SnR_2(DAPTSC)]$ . The phenyl derivative crystallizes as  $[SnPh_2(DAPTSC)] \cdot 2DMF$  in the  $P2_1/n$  space group, with lattice constants:  $a=9.753(1)$ ,  $b=18.962(1)$ ,  $c=17.923(3)$  Å,  $\beta=97.93(1)^\circ$ ,  $Z=4$  and  $R=0.035$ . The molecular complex is pentagonal bipyramidal, with the five donor atoms of the ligand in the pentagonal plane and the two phenyl groups in the axial positions. A comparative study based on the spectral properties (IR, Mössbauer and  $^1H$ ,  $^{13}C$  and  $^{119}Sn$  NMR spectroscopy) of the two complexes suggests a similar structure for  $[SnMe_2(DAPTSC)]$ .

**Key words:** Crystal structures; Tin complexes; Organotin complexes; Thiosemicarbazone complexes

## Introduction

Thiosemicarbazones were the first true antiviral substances to be synthesized [1] and have a wide range of pharmacological [1] and analytical applications [2]. The observed influence of certain metals on the biological activity of these compounds and their intrinsic interest as multidentate ligands, have led to extensive investigation of their coordination chemistry [3]. In particular, much research has been done on N-heterocyclic thiosemicarbazones, including 2-formylpyridine and 2-acetylpyridine thiosemicarbazones and their derivatives [3]. Surprisingly, little attention has been paid to related bis(thiosemicarbazones) [3] with promising coordination properties such as 2,6-diacetylpyridine bis(thiosemicarbazone) ( $H_2DAPTSC$ ) [4].



As part of a research programme devoted to the exploration of the chemistry and the pharmacological activity of diorganotin(IV) derivatives of thiosemicarbazones [5], in this work we synthesized the complexes  $[SnR_2(DAPTSC)]$  ( $R=Me, Ph$ ), the structures of which were characterized by X-ray diffraction ( $R=Ph$ ) and

\*Author to whom correspondence should be addressed.

IR, Mössbauer and  $^1\text{H}$ ,  $^{13}\text{C}$  and  $^{119}\text{Sn}$  NMR spectroscopy. These derivatives are the first complexes of 2,6-diacetylpyridine bis(thiosemicarbazone) with organometallic compounds to be reported, and  $[\text{SnPh}_2(\text{DAPTSC})]$  seems to be the only  $\text{DAPTSC}^{2-}$  complex other than  $[\text{Bi}(\text{DAPTSC})(\text{N}_3)]$  [4a] to have been studied by X-ray crystal analysis. Since structural data are available for organotin(IV) [6] and tin(IV) [7] derivatives of 2,6-diacetylpyridine bis(semicarbazone) and closely related ligands the present report allows evaluation of the electronic and steric effects obtained by substituting sulfur for oxygen in the coordination sphere of the tin atom. Finally, note that this appears to be the first report of the Mössbauer and  $^{119}\text{Sn}$  NMR behaviour of seven-coordinated diorganotin(IV) complexes with an equatorial S,N,N,N,S kernel.

## Experimental

Thiosemicarbazide (Merck), 2,6-diacetylpyridine (Aldrich), dimethyltin(IV) dichloride and diphenyltin(IV) dichloride (Aldrich) were used as supplied. Dimethyltin(IV) and diphenyltin(IV) oxides were obtained from dimethyl- and diphenyltin(IV) dichloride by using a procedure similar to that outlined in ref. 8 for  $\text{SnMe}_2\text{O}$ .  $\text{H}_2\text{DAPTSC}$  was prepared by the procedure of Mohan *et al.* [4e] using EtOH as solvent. Elemental analyses were performed with a Carlo Erba 1108 analyser. Melting points were determined with a Büchi apparatus. IR, NMR and Mössbauer spectra were recorded as before [5].

### Synthesis of $[\text{SnMe}_2(\text{DAPTSC})]$

0.25 g (1.5 mmol) of dimethyltin(IV) oxide was added to a solution of  $\text{H}_2\text{DAPTSC}$  (0.47 g, 1.5 mmol) in DMF (50 ml). The mixture was stirred until a clear solution was obtained, and then left standing for slow evaporation of the solvent, which gave a microcrystalline orange–yellow solid. M.p. 238 °C (decomposition). *Anal.* Found: C, 34.3; H, 4.2; N, 21.2. Calc. for  $\text{C}_{13}\text{H}_{19}\text{N}_7\text{S}_2\text{Sn}$ : C, 34.2; H, 4.2; N, 21.5%.

### Synthesis of $[\text{SnPh}_2(\text{DAPTSC})] \cdot 2\text{DMF}$

0.37 g (1.3 mmol) of diphenyltin(IV) oxide was added to a solution of  $\text{H}_2\text{DAPTSC}$  (0.40 g, 1.3 mmol) in DMF (50 ml). The mixture was heated at 80 °C for 3 h. After cooling and filtering, the clear solution was left standing and a crystalline orange–yellow solid formed. M.p. 300 °C (decomposition). *Anal.* Found: C, 47.6; H, 5.0; N, 16.9. Calc. for  $\text{C}_{29}\text{H}_{37}\text{N}_9\text{O}_2\text{S}_2\text{Sn}$ : C, 47.8; H, 4.6; N, 17.2%.

### X-ray data collection and reduction

A crystal of  $[\text{SnPh}_2(\text{DAPTSC})] \cdot 2\text{DMF}$  was mounted on a glass fibre and used for data collection in an

Enraf-Nonius CAD4 four-circle diffractometer [9]. Cell constants and an orientation matrix for data collection were obtained by least-squares refinement of the diffraction data from 25 reflections in the range of  $18.96 < \theta < 23.96^\circ$ . Data were collected at 293 K using Cu  $K\alpha$  radiation ( $\lambda = 1.54056 \text{ \AA}$ ) and the  $\omega/2\theta$  scan technique, and they were corrected for Lorentz and polarization effects. An empirical absorption correction was made [10]. A summary of the crystal data, experimental details and refinement results is listed in Table 1.

### Structure solution and refinement

The structure was solved by direct methods [11], which revealed the positions of all non-hydrogen atoms, and refined on  $F$  by a full-matrix least-squares procedure using anisotropic displacement parameters for all non-hydrogen atoms. The hydrogen atoms of  $\text{DAPTSC}^{2-}$  were located on a difference Fourier map and those of the DMF methyl groups were calculated; all the hydrogens were then included in the structure factor calculations as fixed contributions ( $B_{\text{iso}} = 4.0 \text{ \AA}^2$ ), but their positional parameters were not refined. A secondary extinction correction [12] was applied. When all shift/e.s.d. ratios were less than 0.001, the refinement converged to the agreement factors listed in Table 1. Atomic scattering factors were taken from ref. 13. Molecular graphics were by SCHAKAL [14].

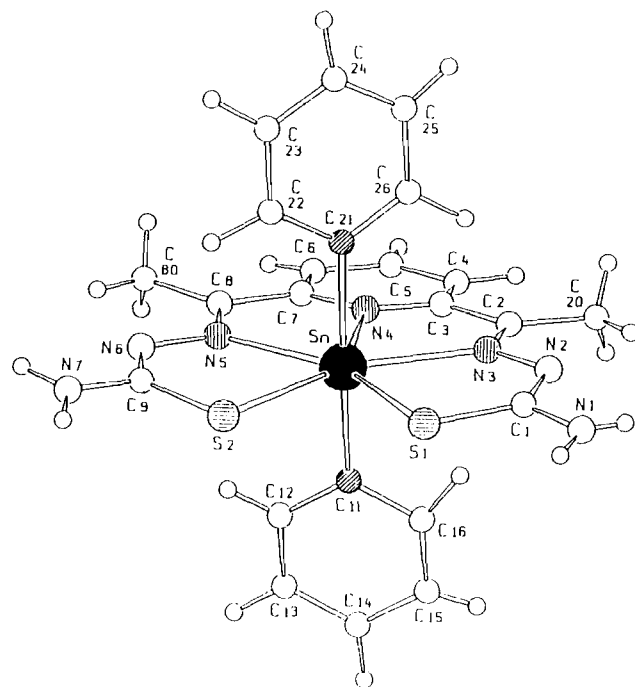


Fig. 1. Perspective view of  $[\text{SnPh}_2(\text{DAPTSC})] \cdot 2\text{DMF}$  showing the atom numbering scheme (DMF not shown).

TABLE 1. Crystal data, data collection and structure refinement parameters of  $[\text{SnPh}_2(\text{DAPTSC})] \cdot 2\text{DMF}$ 

Crystal shape	Prismatic
Size (mm)	0.40 × 0.05 × 0.10
Chemical formula	$\text{C}_{29}\text{H}_{37}\text{N}_9\text{O}_2\text{S}_2\text{Sn}$
Formula weight	726.50
Crystal system	monoclinic
Space group	$P2_1/n$
Unit cell dimensions	
<i>a</i> (Å)	9.753(1)
<i>b</i> (Å)	18.962(1)
<i>c</i> (Å)	17.923(3)
β (°)	97.93(1)
Volume of unit cell (Å <sup>3</sup> )	3282.8(6)
Z	4
<i>D</i> <sub>x</sub> (g cm <sup>-3</sup> )	1.470
<i>F</i> (000)	1488
Linear absorption coefficient (cm <sup>-1</sup> )	78.384
Absorption corrections: min./max./av.	0.876/1.271/1.002
Max. value of (sin θ)/λ reached in intensity measurement (Å <sup>-1</sup> )	0.605
Range of <i>h</i> , <i>k</i> , <i>l</i>	0 → 11, 0 → 22, -21 → 21
Standard reflections	0, -9, -1; 0, -9, 1; 3, -3, 0
Interval standard reflections measured (s)	3600
Total no. reflections measured, θ range (°)	6309, 5–69
No. unique reflections; <i>R</i> <sub>int</sub>	5617; 0.022
No. observed reflections	4501
Criterion for observed reflections	$I > 3\sigma(I)$
Weighting scheme	$1/\sigma^2(F)$
Parameters refined	389
Value of <i>R</i>	0.035
Value of <i>R</i> <sub>w</sub>	0.038
Ratio of max. LS shift to e.s.d. (Δ/σ)	0.001
Max. Δρ in final difference electron density map (e Å <sup>-3</sup> )	0.554
Error in an observation of unit weight	2.115
Secondary extinction coefficient	$3.700 \times 10^{-7}$

## Results and discussion

### Crystal structure of $[\text{SnPh}_2(\text{DAPTSC})] \cdot 2\text{DMF}$

Figure 1 shows the pentagonal bipyramidal nature of the complex. Atomic positions, interatomic distances and angles are given in Tables 2, 3 and 4. The tin atom is surrounded equatorially by the DAPTSC<sup>2-</sup> anion, and the two phenyl groups occupy the axial position. The DAPTSC<sup>2-</sup> anion is approximately planar ( $\chi^2 = 40.6$  when the two phenyl groups are not considered) and the Sn atom lies only 0.021(1) Å out of the least-squares plane through S(1), N(3), N(4), N(5) and S(2) which have an average deviation of 0.027(7) Å from this plane. These donors do not, however, form a regular pentagon as is evidenced by the lengths S(1)–N(3) (2.9668(6)), N(3)–N(4) (2.670(5)), N(4)–N(5) (2.664(6)), N(5)–S(2) (2.967(5)) and S(2)–S(1) (3.350(4) Å); the non-linearity of the fragment C(11)–Sn–C(21) (166.9(2)°) constitutes further distortion from a regular pentagonal bipyramidal coordination polyhedron. The phenyl groups are planar ( $\chi^2 = 10.1$  and 5.4 for C(11), C(12), C(13), C(14), C(15), C(16) (Ph(1)) and C(21), C(22), C(23), C(24), C(25), C(26) (Ph(2)), respectively),

and the dihedral angle between them is 28.8(2)°. Ph(2) is nearly normal to the ligand plane (dihedral angle 87.1(1)°), but Ph(1) forms a dihedral angle of 78.8(1)° with it.

As in  $[\text{Fe}(\text{H}_2\text{DAPTSC})(\text{NCS})_2]$  [4h] the coordination of the ligand is more symmetric than in  $[\text{Bi}(\text{DAPTSC})(\text{N}_3)]$  [4a]. The two S–Sn distances are similar, as are the N(3)–Sn and N(5)–Sn distances. Only the N(4)–Sn bond is clearly shorter than the other two nitrogen–tin bonds, pulling the metallic centre towards the pyridine ring along a hypothetical line bisecting the equatorial girdle. This symmetry is also apparent in the distances and angles of the two thiosemicarbazone arms (Tables 3 and 4). Differences in these parameters are, in general, inside or close to the e.s.d. range. Sn–S and Sn–N<sub>hydrazinic</sub> bond distances are longer than in  $[\text{SnR}_2(\text{L})]$  (R = Me, Ph; L = salicylaldehydethiosemicarbazone) [5], probably due to the increase in the number of donor atoms coordinated to the metallic centre and to the steric limitations imposed by DAPTSC<sup>2-</sup> on its pentacoordination geometry. Nevertheless, the influence of the latter factor must be slight because some flexibility of the ligand backbone

TABLE 2. Positional parameters for [SnPh<sub>2</sub>(DAPTSC)]·2DMF, with e.s.d.s in parentheses

Atom	<i>x</i>	<i>y</i>	<i>z</i>	<i>B</i> (Å <sup>2</sup> )
Sn	0.18864(3)	0.72212(1)	0.01541(2)	2.310(5)
S1	0.2847(1)	0.82666(6)	-0.05495(7)	3.43(2)
S2	0.1093(1)	0.82686(6)	0.09309(7)	3.33(2)
O30	0.5950(6)	0.4718(3)	0.3245(3)	7.9(1)
O40	0.5300(5)	0.0299(2)	0.1491(3)	6.6(1)
N1	0.4228(4)	0.8228(2)	-0.1691(2)	3.24(8)
N2	0.3640(4)	0.7127(2)	-0.1350(2)	2.83(8)
N3	0.3053(4)	0.6733(2)	-0.0840(2)	2.50(7)
N4	0.1866(4)	0.5973(2)	0.0150(2)	2.54(7)
N5	0.0653(4)	0.6735(2)	0.1119(2)	2.67(8)
N6	-0.0016(4)	0.7132(2)	0.1605(2)	2.83(8)
N7	-0.0552(5)	0.8229(2)	0.1960(2)	3.80(9)
N30	0.4095(6)	0.5370(3)	0.3403(4)	6.7(2)
N40	0.5859(5)	-0.0732(2)	0.0999(3)	4.6(1)
C1	0.3598(5)	0.7819(3)	-0.1231(2)	2.72(9)
C2	0.3213(5)	0.6050(3)	-0.0879(3)	2.85(9)
C3	0.2597(5)	0.5627(2)	-0.0317(3)	2.80(9)
C4	0.2778(6)	0.4899(3)	-0.0259(3)	3.6(1)
C5	0.2172(6)	0.4537(3)	0.0281(3)	4.2(1)
C6	0.1435(6)	0.4901(3)	0.0755(3)	3.8(1)
C7	0.1296(5)	0.5628(3)	0.0680(3)	2.80(9)
C8	0.0551(5)	0.6053(3)	0.1188(2)	2.81(9)
C9	0.0128(5)	0.7825(3)	0.1521(2)	2.78(9)
C11	0.3800(5)	0.7040(2)	0.0911(3)	2.60(9)
C12	0.3811(5)	0.7001(3)	0.1680(3)	3.7(1)
C13	0.5046(6)	0.6876(4)	0.2156(3)	4.8(1)
C14	0.6275(6)	0.6804(3)	0.1872(3)	4.5(1)
C15	0.6279(5)	0.6854(3)	0.1115(3)	4.3(1)
C16	0.5054(5)	0.6976(3)	0.0627(3)	3.4(1)
C20	0.3987(7)	0.5711(3)	-0.1439(3)	5.3(1)
C21	-0.0061(5)	0.7141(2)	-0.0600(2)	2.57(9)
C22	-0.1266(5)	0.7401(3)	-0.0368(3)	3.2(1)
C23	-0.2540(5)	0.7362(3)	-0.0840(3)	3.8(1)
C24	-0.2605(5)	0.7049(3)	-0.1540(3)	3.8(1)
C25	-0.1432(6)	0.6793(3)	-0.1772(3)	4.0(1)
C26	-0.0156(5)	0.6842(3)	-0.1305(3)	3.5(1)
C30	0.5353(9)	0.5186(4)	0.3527(6)	8.5(2)
C31	0.330(1)	0.4998(7)	0.2778(7)	11.9(4)
C32	0.345(1)	0.5915(6)	0.3695(7)	17.9(4)
C40	0.5853(7)	-0.0045(3)	0.1044(3)	5.1(1)
C41	0.6549(8)	-0.1105(4)	0.0457(4)	6.6(2)
C42	0.526(1)	-0.1147(4)	0.1516(5)	8.9(2)
C80	-0.0238(6)	0.5706(3)	0.1744(3)	4.0(1)

Anisotropically refined atoms are given in the form of the isotropic equivalent displacement parameter defined as:  $(4/3)[a^2B(1,1) + b^2B(2,2) + c^2B(3,3) + ab(\cos \gamma)B(1,2) + ac(\cos \beta)B(1,3) + bc(\cos \alpha)B(2,3)]$ .

is indicated by the structural data for the complex [Sn(DAPSC)Cl<sub>2</sub>]·2H<sub>2</sub>O (DAPSC<sup>2-</sup> = 2,6-diacetylpyridine bis(semicarbazone)) [7], in which the apical Ph groups of [SnPh<sub>2</sub>(DAPTSC)]·2DMF are replaced by two Cl atoms and its two sulfur atoms by oxygen atoms: not only are the Sn–X distances (X = O, S) shorter in the semicarbazone complex, but also all the other equatorial Sn–ligand distances, in spite of which, the angles subtended at the tin atom are fairly similar in

TABLE 3. Bond distances (Å) in [SnPh<sub>2</sub>(DAPTSC)]·2DMF

Sn–S1	2.593(1)	C2–C3	1.480(7)
Sn–S2	2.603(1)	C2–C20	1.483(9)
Sn–N3	2.427(4)	C22–C23	1.406(7)
Sn–N4	2.368(3)	C23–C24	1.380(8)
Sn–N5	2.421(4)	C24–C25	1.360(8)
Sn–C11	2.178(4)	C25–C26	1.403(7)
Sn–C21	2.179(4)	C3–C4	1.394(7)
S1–C1	1.731(5)	C4–C5	1.384(9)
S2–C9	1.729(5)	C5–C6	1.373(8)
N1–C1	1.341(6)	C6–C7	1.390(7)
N2–N3	1.365(5)	C7–C8	1.479(7)
N2–C1	1.331(7)	C8–C80	1.493(7)
N3–C2	1.307(6)	C11–C12	1.380(7)
N4–C3	1.343(6)	C11–C16	1.393(8)
N4–C7	1.337(6)	C12–C13	1.398(7)
N5–N6	1.381(5)	C13–C14	1.372(9)
N5–C8	1.306(7)	C14–C15	1.361(8)
N6–C9	1.333(6)	C15–C16	1.400(7)
N7–C9	1.338(6)	C21–C22	1.391(7)
		C21–C26	1.377(7)

TABLE 4. Bond angles (°) in [SnPh<sub>2</sub>(DAPTSC)]·2DMF

S1–Sn–S2	80.26(5)	S2–C9–N7	115.9(4)
S1–Sn–N3	72.4(1)	N6–C9–N7	115.5(4)
S1–Sn–N4	140.0(2)	C12–C11–C16	118.3(4)
S1–Sn–N5	152.49(9)	C11–C12–C13	120.4(5)
S1–Sn–C11	95.0(1)	C12–C13–C14	121.0(5)
S1–Sn–C21	95.4(1)	C13–C14–C15	119.0(5)
S2–Sn–N3	152.60(9)	C14–C15–C16	121.1(5)
S2–Sn–N4	139.7(2)	C11–C16–C15	120.2(5)
S2–Sn–N5	72.23(9)	N2–N3–C2	116.3(4)
S2–Sn–C11	94.6(1)	C3–N4–C7	120.8(4)
S2–Sn–C21	95.1(1)	N6–N5–C8	115.6(4)
N3–Sn–N4	67.8(1)	N5–N6–C9	113.5(4)
N3–Sn–N5	135.2(1)	S1–C1–N1	115.2(4)
N3–Sn–C11	87.1(1)	S1–C1–N2	128.5(4)
N3–Sn–C21	88.5(1)	N1–C1–N2	116.4(4)
N4–Sn–N5	67.5(1)	N3–C2–C3	116.1(4)
N4–Sn–C11	81.5(1)	N3–C2–C20	122.8(4)
N4–Sn–C21	85.5(1)	C3–C2–C20	121.1(4)
N5–Sn–C11	87.9(1)	N4–C3–C2	117.3(5)
N5–Sn–C21	86.6(1)	N4–C3–C4	120.7(4)
C11–Sn–C21	166.9(2)	C2–C3–C4	122.0(5)
N3–N2–C1	114.0(4)	C3–C4–C5	118.9(5)
N4–C7–C6	120.6(5)	C4–C5–C6	119.5(5)
N4–C7–C8	117.3(5)	C5–C6–C7	119.5(5)
C6–C7–C8	122.1(4)	C22–C21–C26	118.0(5)
N5–C8–C7	115.6(4)	C21–C22–C23	121.0(4)
N5–C8–C80	123.6(4)	C22–C23–C24	119.7(5)
C7–C8–C80	120.9(4)	C23–C24–C25	119.8(5)
S2–C9–N6	128.6(4)	C24–C25–C26	120.6(5)
		C21–C26–C25	121.1(5)

the two complexes (as expected, the maximum discrepancy is for the X–Sn–X angle which is 2.3° wider in [SnPh<sub>2</sub>(DAPTSC)]·2DMF). This is achieved by the ‘internal’ angles of the DAPTSC<sup>2-</sup> backbone being wider than those of DAPSC<sup>2-</sup>, the only exceptions being C(1)–N(2)–N(3) and C(9)–N(6)–N(5) for which

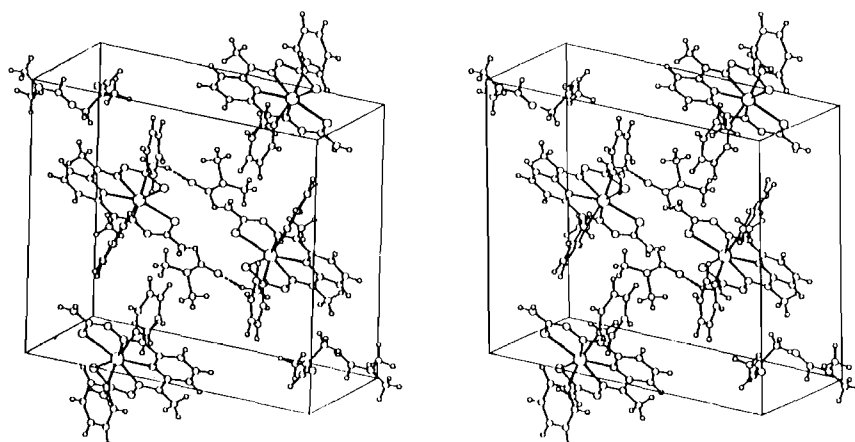


Fig. 2. Stereoview of the unit cell packing.

the  $sp^2$  lone pairs on N(2) and N(6) may hinder the widening of the angle.

DMF molecules are linked to the amino groups by the following hydrogen bonds (Fig. 2):  $N(1)\dots O(40)^i = 2.847(6)$  Å,  $N(1)-H(10)\dots O(40)^i = 1.92(9)$  Å,  $N(1)-H(10)-O(40)^i = 158.9(8)^\circ$  ( $i = 1-x, 1-y, z$ );  $N(7)\dots O(30)^{ii} = 2.867(7)$  Å,  $N(7)-H(70)\dots O(30)^{ii} = 1.986(5)$  Å,  $N(7)-H(70)-O(30)^{ii} = 153.7(6)^\circ$  ( $ii = 0.5-x, y-0.5, 0.5-z$ ).

#### Infrared spectroscopy

Table 5 lists the main IR bands of the ligand and its complexes (the former assigned following previous work [4c-e] and by comparison with pyridine-2-carbaldehyde thiosemicarbazones) [15].

The IR spectrum of  $DAPTSC^{2-}$  in  $[SnPh_2(DAPTSC)] \cdot 2DMF$  differs in several respects from that of the free

ligand. Coordination of the pyridine ring [16] shifts one of the ring stretching bands to lower frequencies (though the position of the other is practically unchanged) and  $\gamma(C-H)$ ,  $\delta(\text{ring})$  and  $\gamma(\text{ring})$  are all shifted to higher wavenumbers. Coordination of the azomethine N atom, as in other thiosemicarbazones [17], slightly shifts the ligand  $\nu(C=N)$  band to higher frequencies while S-coordination dampens the ligand  $\nu(C=S)$  bands and shifts them to lower frequencies. (Mohan *et al.* [4e] attributed to  $\nu(N-N)$  the  $H_2DAPTSC$  band at  $1090\text{ cm}^{-1}$ ,  $1080\text{ cm}^{-1}$  in their spectrum, and suggested that its shift to lower wavenumbers upon complexation was due to coordination of the azomethine nitrogen atom). Finally,  $\nu(N-H)$  is shifted to slightly lower frequencies.

The spectrum of the methyl derivative lacks the DMF bands present in that of the phenyl derivative (not shown in Table 5), but has a similar ligand vibration

TABLE 5. Main IR bands of the ligand and its complexes ( $\text{cm}^{-1}$ )

$H_2DAPTSC$	$[SnMe_2(DAPTSC)]$	$[SnPh_2(DAPTSC)] \cdot 2DMF$	Assignment
3430m	3360m	3360m	$\nu(NH)$
3340m	3260m, b	3300m, b	
3270m	3120m, b	3180m, b	
3160m			
1600vs	1610vs	1620vs	$\delta(NH)$
1570m	1585m	1580m	$\nu(C=N)$
1490s	1450s, b	1470sh	$\nu(\text{ring})$
		1460s	
1440s	1440sh	1430m	$\nu(\text{ring})$
		1420m	
1100s	1100w		$\nu(C=S)$
1090sh	1040m	1060m	$\nu(C=S)$
830m	780m	780m	$\nu(C=S)$
	770m		
725m	735m	735m	$\gamma(C-H)$
615m	640m	660m	$\delta(\text{ring})$
		640m	
420m	450m	460m, b	$\gamma(\text{ring})$

pattern. Thus in  $[\text{SnMe}_2(\text{DAPTSC})]$  the ligand must have the same pentadentate coordination as in  $[\text{SnPh}_2(\text{DAPTSC})] \cdot 2\text{DMF}$ . Note that  $\nu(\text{N-H})$  also appears at similar positions in the two spectra, so the methyl derivative probably has intermolecular hydrogen bond involving the  $\text{NH}_2$  group. Both spectra show bands attributable to the C-Sn-C fragment (at 270 (m) and 220(sh)  $\text{cm}^{-1}$  in the phenyl derivative and 490(s)  $\text{cm}^{-1}$  in the methyl derivative) and others that are probably contributed to by  $\nu(\text{Sn-N}(\text{azomethine}))$ ,  $\nu(\text{Sn-S})$  or  $\nu(\text{Sn-N}(\text{py}))$  (in the proximity of 370, 300 and 230  $\text{cm}^{-1}$ , respectively).

#### Mössbauer spectroscopy

The Mössbauer spectra of the two  $[\text{SnR}_2(\text{DAPTSC})]$  complexes present a single quadrupole split doublet; the two peaks are slightly asymmetric, but the linewidths are narrow enough to exclude a second component. The quadrupole splitting values (Table 6) indicate a *trans* arrangement of the two R groups, with C-Sn-C angles less than  $180^\circ$ .

The *PQS* values proposed [6b] for the R groups of seven-coordinated diorganotin(IV) complexes on the basis of X-ray and Mössbauer data for  $[\text{SnEt}_2(\text{dapt})]$  ( $\text{H}_2\text{dapt} = 2,6$ -diacetylpyridine bis(2-thenoylhydrazone)) [6b],  $[\text{SnPr}_2(\text{daps})]$  ( $\text{H}_2\text{daps} = 2,6$ -diacetylpyridine bis(salicyloylhydrazone)) [6b] and  $[\text{SnPh}_2(\text{dapa})]$  ( $\text{H}_2\text{dapa} = 2,6$  diacetylpyridine bis(2-aminobenzoylhydrazone)) [6b] were used to quantify the deviation of the C-Sn-C bond angles from the ideal  $180^\circ$ . The angle calculated for the phenyl derivative,  $152^\circ$ , is approximately  $15^\circ$  narrower than the value obtained by X-ray diffraction (*vide supra*), and a similar value ( $154^\circ$ ) was obtained for the methyl complex. The only differences between  $\text{DAPTSC}^{2-}$  and the hydrazone complexes that might account for this discrepancy is that the hydrazone complexes have oxygen instead of sulfur as terminal donating atoms and bulky lipophilic benzene rings instead of small hydrophilic amino groups. The difference in electronegativity between oxygen and sulfur can alter both the electron density at the tin nucleus (see the discussion of NMR results below) and the distribution between the s and p orbitals (with consequences on the isomer shift and quadrupole splitting), while the difference in size and lipophilicity of the terminal organic group may influence its position in

the crystal structure of the compounds and may also contribute to the observed decrease in the values of the isomer shift. If the influence of substituent electronegativity on the quadrupole splitting is also significant, the applicability of previously reported [6b] *PQS* values for seven-coordinated diorganotin(IV) complexes must be limited (in fact, the *PQS* value obtained for {aryl} when the structural and Mössbauer data for  $[\text{SnPh}_2(\text{DAPTSC})]$  are used ( $-0.88 \text{ mm s}^{-1}$ ) clearly differs from the value previously calculated ( $-0.78 \text{ mm s}^{-1}$ ) using  $[\text{SnPh}_2(\text{dapa})]$  data [6b]). It is evident that, as Carini *et al.* [6b] pointed out, more data are necessary before confidence can be placed in this approach to the estimation of the C-Sn-C angle in diorganotin(IV) complexes with very large coordination numbers.

#### $^1\text{H}$ , $^{13}\text{C}$ and $^{119}\text{Sn}$ spectroscopy

The complexes are soluble in DMSO and in DMF. Their NMR signals in DMSO (or DMSO- $d_6$ ) are listed in Table 7. The corresponding data for the ligand part of the spectra in DMF (or DMF- $d_7$ ) are similar (differences  $\leq 0.1$  ppm in the proton spectra and  $\leq 1.25$  ppm in the  $^{13}\text{C}$  NMR spectra) and are not included in Table 7.

The changes in the spectra of  $\text{H}_2\text{DAPTSC}$  under complexation are closely related to those observed when pyridine-2-carbaldehyde thiosemicarbazone (PyTSC) becomes S, N(3), N(4)-coordinated [15, 18]. In the  $^1\text{H}$  NMR spectrum the following modifications are observed when the complexes  $[\text{SnR}_2(\text{DAPTSC})]$  form: (i) the N(2)/N(6)-H signal disappears as a consequence of double deprotonation of the ligand; (ii) the protons of the  $-\text{NH}_2$  groups are shielded and merge in a single signal; (iii) only the proton C(5)-H is deshielded in the complexes in accordance with the trend observed for pyridine protons under nitrogen protonation [19], C(4)-H and C(6)-H being shielded by complexation. As has been suggested for other pyridine-related thiosemicarbazones [15, 18], this dissimilar behaviour of the pyridine ring hydrogens may be related to changes in the conformation of the thiosemicarbazone 'arms' of the ligand when complexes form, different magnetic environments being created for the protons closer to the arms.

Regarding the  $^{13}\text{C}$  NMR spectra, C(1)/C(9), unlike C(1) in the cadmium(II) complex of PyTSC, are more shielded in  $[\text{SnR}_2(\text{DAPTSC})]$  than in  $\text{H}_2\text{DAPTSC}$ . In this case, the shielding influence of the tautomeric (thione-thiol) rearrangement of the ligand thiamide group upon deprotonation and metallation overcomes the inductive effect of the sulfur-metal bond which seems to be weaker than in  $[\text{Cd}(\text{PyTSC})_2]$ . All the other carbon signals behave in the same way as for the cadmium compound [15]: C(2)/C(8) and C(3)/C(7) are shielded upon complexation and C(4)/C(6) and C(5)

TABLE 6.  $^{199}\text{Sn}$  Mössbauer data<sup>a</sup> for the complexes

Compound	<i>IS</i> <sup>b</sup> (mm s <sup>-1</sup> )	<i>QS</i> (mm s <sup>-1</sup> )	<i>F</i>
$[\text{SnMe}_2(\text{DAPTSC})]$	1.41	3.58	0.88
$[\text{SnPh}_2(\text{DAPTSC})] \cdot 2\text{DMF}$	1.22	2.84	0.88

<sup>a</sup>Collected at 80.0 K. <sup>b</sup>Relative to room temperature  $\text{SnO}_2$ .

TABLE 7. More significant  $^1\text{H}$ ,  $^{13}\text{C}$  and  $^{119}\text{Sn}$  NMR data

Compound	N(2)H	N(1)H <sub>2</sub>	C(4)H/C(6)H	C(5)H	C(20)H <sub>3</sub> /C(80)H <sub>3</sub>	Sn-R	$^2J(^1\text{H-Sn})$	DMF
H <sub>2</sub> DAPTSC	10.32, s(2)	8.41, s(2) 8.16, s(2)	8.42, d(2)	7.76, t(1)	2.43, s(6)			
[SnMe <sub>2</sub> (DAPTSC)]		7.07, sb(4)	7.89, d(2)	8.17, t(1)	2.49, s	0.49, s(6)	115.3/110.5	2.89, s(6)
[SnPh <sub>2</sub> (DAPTSC)]·2DMF		7.37, sb(4)	7.82, d(2)	8.04, t(1)	2.55, s(6)	7.23(o), m(4) 7.00(m, p), m(6)		2.72, s(6) 7.94, s(2)
	C(1)/C(9)	C(3)/C(7)	C(2)/C(8)	C(4)/C(6)	C(5)	C(20)/C(80)	Sn-C	DMF
H <sub>2</sub> DAPTSC	179.20	153.58	148.20	120.84	136.64	11.96	26.36	
[SnMe <sub>2</sub> (DAPTSC)]	177.04	148.65	143.88	121.89	141.01	13.82		1169.8/ 1122.0
[SnPh <sub>2</sub> (DAPTSC)]·2DMF	177.20	148.06	144.68	122.13	141.14	14.10	160.27(i) 131.52(o) 127.43(m) 126.69(p)	30.71 35.70 162.37
								$\delta(^{119}\text{Sn})$
								-393
								-453

deshielded. Note that the signals of the pyridine ring atoms, whose magnetic environment is unlikely to be significantly affected by conformational changes in the thiosemicarbazone arms, behave in the same way as when the pyridine nitrogen atom becomes protonated (*ortho* carbons becoming shielded and *meta* and *para* carbons deshielded [19]).

With regard to the ligand signals, the spectral behaviour of [SnMe<sub>2</sub>(DAPTSC)] is similar to that described above for the phenyl derivative, suggesting that the coordination mode of DAPTSC<sup>2-</sup> is the same in the two complexes in solution as well as in solid state. However, the simpler spectrum of the methyl derivative allows observation of satellite peaks flanking the signal for C(2)/C(8) with separation of 24.2 Hz. These satellites may plausibly be attributed to Sn-C coupling via the Sn-N(3)/N(5) bonds.

To summarize, in spite of the donor character of the solvents used in this study, the ligand signals suggest that DAPTSC<sup>2-</sup> maintains its pentadentate behaviour in DMSO and DMF solutions. This conclusion is supported by the value of  $^2J(^1\text{H-}^{119}\text{Sn})$  in [SnMe<sub>2</sub>(DAPTSC)] (Table 7), which is in the range considered typical for seven-coordinate species [20]. Substitution of this coupling constant in the Lockhart-Manders equation [21] leads to prediction of an impossible C-Sn-C angle (197°), but the large  $J$  value, like those of other seven-coordinated dimethyltin(IV) complexes [22] measured in DMSO, is taken to indicate an approximately linear C-Sn-C fragment.

Though all the  $^1\text{H}$  and  $^{13}\text{C}$  NMR information points to the structural characteristics of the complexes in the solid state being maintained in DMSO (or DMF) solution (and hence, in particular, to the heptacoordination of the tin atom being conserved), the tin nuclide is less shielded in DAPTSC<sup>2-</sup> compounds than in seven-coordinate diorganotin(IV) derivatives possessing 3N, 2O- or 2N, 3O-pentadentate ligands [6, 20, 22],  $\delta(^{119}\text{Sn})$  lying as much as *c.* 100 ppm farther downfield in the case of the phenyl derivative. These differences are probably due to the sulfur atoms having a smaller shielding effect on the tin nuclide than oxygen atoms; a similar difference between the effects of S and O atoms has been reported for the Cd nuclide [23], among others. Five- and six-coordinate dialkyltin(IV) mono- or bis(thiosemicarbazones) also have relatively deshielded  $^{119}\text{Sn}$  signals, though shielding rises steadily, as expected [24], as coordination number increases (e.g. for five-coordinate tin in [SnMe<sub>2</sub>(salicylaldehydethiosemicarbazone)],  $\delta(^{119}\text{Sn}) = -123$  ppm [25]; for six-coordinated tin in [SnEt<sub>2</sub>{benzyl} bis(thiosemicarbazone)]  $\delta(^{119}\text{Sn}) = -305$  ppm [25]; for seven-coordinated tin in [SnMe<sub>2</sub>(DAPTSC)],  $\delta(^{119}\text{Sn}) = -393$  ppm). Thus the chemical shift of tin in diorganotin complexes appears to depend not only on

coordination number, but also on the identity of the donor atoms in the coordination sphere.

Finally, note that the carbon atoms of the tin-bonded methyl groups in [SnMe<sub>2</sub>(DAPTSC)] and the *ipso* carbons of the phenyl groups in [SnPh<sub>2</sub>(DAPTSC)]·2DMF are strongly deshielded (the identity of the Sn–Me signal was confirmed using a heteronuclear COSY experiment), possibly due to some deshielding influence of the  $\pi$  charge delocalized along the DAPTSC<sup>2-</sup> ligand.

### Acknowledgement

We thank the DGICYT (Spain) for financial support under Project PS90-0195.

### References

- 1 C.J. Pfau, *Handb. Exp. Pharmacol.*, **61** (1982) 147.
- 2 R.B. Sing, B.S. Garg and R.P. Singh, *Talanta*, **25** (1978) 619.
- 3 D.X. West, A.E. Liberta, S.B. Padhye, R.C. Chitake, P.B. Sonawane, A.S. Kumbhar and R.G. Yerande, *Coord. Chem. Rev.*, **123** (1993) 49; D.X. West, S.B. Padhye and P.B. Sonawane, *Struct. Bonding (Berlin)*, **76** (1991) 1; S. Padhye and G.B. Kauffman, *Coord. Chem. Rev.*, **63** (1985) 127; M.J.M. Campbell, *Coord. Chem. Rev.*, **15** (1975) 279.
- 4 (a) L.P. Battaglia, A.B. Corradi, C. Pelizzi, G. Pelosi and P. Tarasconi, *J. Chem. Soc., Dalton Trans.*, (1990) 3857; (b) L.J. Ming, R.B. Lauffer and L. Que, Jr., *Inorg. Chem.*, **29** (1990) 3060; (c) H.D.S. Yadav, S.K. Sengupta and S.C. Tripathi, *Bull. Soc. Chim. Fr.*, (1988) 29; *Acta Chim. Hung.*, **124** (1987) 217; *Bull. Soc. Chim. Fr.*, (1986) 716; (d) V.M. Leovac and V.I. Cesljevic, *Transition Met. Chem.*, **12** (1987) 504; (e) M. Mohan, P. Sharma, M. Kumar and N.K. Jha, *Inorg. Chim. Acta*, **125** (1986) 9; (f) M.P. Martínez-Martínez, M. García-Vargas and J.A. Muñoz-Leyva, *Spectrochim. Acta, Part A*, **42** (1986) 701; (g) F. Castañeda, A. García de Torres and J.M. Cano-Pavón, *Microchem. J.*, **28** (1983) 556; (h) G. Dessy and V. Fares, *Cryst. Struct. Commun.*, **10** (1981) 1025.
- 5 J.S. Casas, A. Sánchez, J. Sordo, A. Vázquez-López, E.E. Castellano, J. Zuckerman-Schpector, M.C. Rodríguez-Argüelles and U. Russo, *Inorg. Chim. Acta*, **216** (1994) 169.
- 6 (a) P. Mazza, M. Orcesi, C. Pelizzi, G. Pelizzi, G. Predieri and F. Zani, *J. Inorg. Biochem.*, **48** (1992) 251; (b) C. Carini, G. Pelizzi, P. Tarasconi, C. Pelizzi, K.C. Molloy and P.C. Waterfield, *J. Chem. Soc., Dalton Trans.*, (1989) 289; (c) D. Delledonne, G. Pelizzi and C. Pelizzi, *Acta Crystallogr., Sect. C*, **43** (1987) 1502; (d) C. Pelizzi, G. Pelizzi and G. Predieri, *J. Organomet. Chem.*, **263** (1984) 9; (e) C. Pelizzi and G. Pelizzi, *J. Chem. Soc., Dalton Trans.*, (1980) 1970.
- 7 S.O. Sommerer and G.J. Palenik, *Inorg. Chim. Acta*, **183** (1991) 217.
- 8 R.S. Tobias, I. Ogrins and B.A. Nevett, *Inorg. Chem.*, **1** (1962) 638.
- 9 B.A. Frenz & Associates Inc., *Structure Determination Package, SDP/VAX V.2.2*, College Station, TX, USA, and Enraf-Nonius, Delft, Netherlands, 1985.
- 10 N. Walker and D. Stuart, *Acta Crystallogr., Sect. A*, **39** (1983) 158.
- 11 G.M. Sheldrick, *SHELXS86*, program for the solution of crystal structures from X-ray diffraction data, University of Göttingen, Germany, 1986.
- 12 W.H. Zachariasen, *Acta Crystallogr.*, **16** (1963) 1139.
- 13 *International Tables for X-ray Crystallography*, Vol. IV, Kynoch, Birmingham, UK, 1974.
- 14 E. Keller, *SCILAKAL*, program for plotting molecular and crystal structures, University of Freiburg, Germany, 1988.
- 15 J.S. Casas, M.V. Castaño, M.S. García-Tasende, I. Martínez-Santamarta, A. Sánchez, J. Sordo, E.E. Castellano and J. Zuckerman-Schpector, *J. Chem. Res. S*, (1992) 324; *M*, (1992) 2626, and refs. therein.
- 16 D.A. Thornton, *Coord. Chem. Rev.*, **104** (1990) 251, and refs. therein.
- 17 A. Macías, M.C. Rodríguez-Argüelles, M.I. Suárez, A. Sánchez, J.S. Casas, J. Sordo and U. Englert, *J. Chem. Soc., Dalton Trans.*, (1989) 1787.
- 18 J.S. Casas, M.V. Castaño, M.C. Rodríguez-Argüelles, A. Sánchez and J. Sordo, *J. Chem. Soc., Dalton Trans.*, (1993) 1253.
- 19 R.J. Pugmire and D.M. Grant, *J. Am. Chem. Soc.*, **90** (1968) 697.
- 20 M. Careri, A. Mangia, G. Predieri and C. Vignali, *J. Organomet. Chem.*, **375** (1989) 39.
- 21 T.P. Lockhart and W.F. Manders, *Inorg. Chem.*, **25** (1986) 892.
- 22 T.P. Lockhart and F. Davidson, *Organometallics*, **6** (1987) 2471.
- 23 P.D. Ellis, in J.B. Lambert and F.G. Riddell (eds.), *The Multinuclear Approach to NMR Spectroscopy*, NATO ASI Series, Reidel, Dordrecht, 1983, Ch. 22, pp. 457–523.
- 24 J. Otera, T. Hinoishi and R. Okawara, *J. Organomet. Chem.*, **202** (1980) C93; J. Otera, *J. Organomet. Chem.*, **221** (1981) 57.
- 25 J.S. Casas, M.V. Castaño, M.C. Rodríguez-Argüelles, A. Sánchez and J. Sordo, unpublished work.